Spatial and temporal Taylor's law in 1D chaotic maps **⊘**

Hiroki Kojima 🕶 🗓 ; Yuzuru Mitsui; Takashi Ikegami



Chaos 31, 033111 (2021)

https://doi.org/10.1063/5.0036892





CrossMark





Spatial and temporal Taylor's law in 1D chaotic maps

Cite as: Chaos 31, 033111 (2021); doi: 10.1063/5.0036892 Submitted: 16 November 2020 · Accepted: 9 February 2021 · Published Online: 2 March 2021





Hiroki Kojima, D Yuzuru Mitsui, and Takashi Ikegami

AFFILIATIONS

The Graduate School of Arts and Sciences, University of Tokyo, 3-8-1 Komaba, Meguro-ku, Tokyo 153-8902, Japan

a)Author to whom correspondence should be addressed: kojima@sacral.c.u-tokyo.ac.jp

ABSTRACT

By using low-dimensional chaotic maps, the power-law relationship established between the sample mean and variance called Taylor's Law (TL) is studied. In particular, we aim to clarify the relationship between TL from the spatial ensemble (STL) and the temporal ensemble (TTL). Since the spatial ensemble corresponds to independent sampling from a stationary distribution, we confirm that STL is explained by the skewness of the distribution. The difference between TTL and STL is shown to be originated in the temporal correlation of a dynamics. In case of logistic and tent maps, the quadratic relationship in the sample mean and variance, called Bartlett's law, is found analytically. On the other hand, TTL in the Hassell model can be well explained by the chunk structure of the trajectory, whereas the TTL of the Ricker model has a different mechanism originated from the specific form of the map.

Published under license by AIP Publishing. https://doi.org/10.1063/5.0036892

Taylor's Law (TL) is a widely held power-law-like behavior between sample mean and sample variance, originally found in the field of population ecology. When the sample mean and sample variance are calculated from a time series, it is called temporal TL (TTL), and when these are calculated from a different time series at a given time, it is called spatial TL (STL). TL has been observed in a variety of fields outside of population ecology, but the mechanism of TL and the relationship between TTL and STL is still unclear. In this paper, we report a new relationship between STL and TTL using four basic one-dimensional chaotic maps, including a logistic map. Specifically, we analytically derive the relationship between TTL and STL from stationary distributions and temporal correlations as a generalization of Cohen and Xu.²² In the case of logistic and tent maps, a quadratic relationship between sample mean and sample variance, called Bartlett's law, was found analytically: the TTL of the Hassell model can be adequately explained by the chunk structure of the trajectory, whereas the TTL of the Ricker model is a different mechanism derived from the shape of the map. We believe that the analysis in this paper may provide clues in the more general case as well.

I. INTRODUCTION

We challenged the unexplained widespread power-law behavior between the sample mean and sample variance, called Taylor's law (TL),1,2 with one-dimensional (1D) chaotic maps. TL was originally found in the field of population ecology and has since been reported more widely, ranging from demographic ecology to prime number distribution,³ complex networks,⁴ and so on.^{5,6} TL expresses that a power-law scaling relationship holds between the sample mean (M) and variance (V) as $V = \alpha M^{\beta}$.

When the data are composed of N trajectories with the total time step *T*, the sample mean and the sample variance can be computed in two ways, spatial and temporal. By denoting the value of nth time steps from the ith trajectory as x_n^i , the spatial mean and variance are defined as

$$M_n = rac{1}{N} \sum_{i=1}^N x_n^i,$$

$$V_n = rac{1}{N} \sum_{i=1}^N \left(x_n^i - M_n
ight)^2,$$

and the temporal mean and variance are defined as

$$M_i = \frac{1}{T} \sum_{n=1}^{T} x_n^i,$$

$$V_i = \frac{1}{T} \sum_{n=1}^{T} (x_n^i - M_i)^2.$$

We call the relationship between the spatial mean and variance as spatial TL (STL) and the temporal mean and variance as temporal TL (TTL).

STL and TTL have been analyzed in several dynamical systems of ecological models. To For example, Ballantyne showed that the exponent of TTL becomes 2 when the solution of the map is linearly scaled by changes in the parameters, and Kilpatrick and Ives used the noisy Ricker model of multiple species to show TTL between the sample mean and variance. Perry found STL in the chaotic regions of the Hassell model controlled by noise, but they provided no analytical explanations. Cohen showed that the exponential growth model satisfies STL with the exponent $\beta=2$ in the limit of large time. 10

In this paper, we investigate both STL and TTL in the chaotic regime of 1D maps, discussing a possible mechanism of both STL and TTL. There are only a few studies that have investigated the relationship of STL and TTL. $^{11-13}$ They use empirical data with a probabilistic model, but no theoretical explanation was provided. We discuss that spatial TL is explained by the skewed distribution function, while temporal TL is dependent on the temporal correlations in a time series. Zhao *et al.* 13 argued that the skewness of the population abundance was an important factor of the exponent β . Although they recognized that the autocorrelation of the time series was important, their main numerical simulations did not consider it. Here, we will show that autocorrelation greatly influenced TL.

II. TL IN 1D CHAOTIC MAPS

We examined four discrete one-dimensional chaotic map systems that basically adopted ecological modelings—i.e., logistic map, tent map, Hassell model, ^{14,15} and Ricker model ^{16,17}—which have been widely used as population models, ^{18,19}

$$x_{n+1} = rx_n(1 - x_n) \ (0 \le x \le 1), \tag{1}$$

$$x_{n+1} = \frac{\mu}{2} - \mu \left| x_n - \frac{1}{2} \right| \ (0 \le x \le 1),$$
 (2)

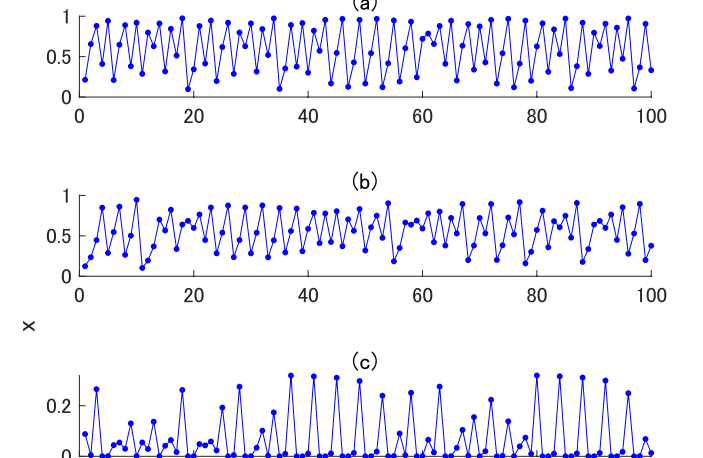
$$x_{n+1} = \frac{\lambda x_n}{\left(1 + \kappa x_n\right)^{\nu}} \ (x \ge 0),\tag{3}$$

$$x_{n+1} = x_n \exp\{r(1 - x_n)\} \ (x \ge 0). \tag{4}$$

The typical chaotic time series generated from these maps are shown in Fig. 1.

In the following analysis, we used the parameter sets r=3.9 (logistic map), $\mu=1.9$ (tent map), $\kappa=10, \nu=12, \lambda=100$ (Hassell model), and r=5 (Ricker model). As we will show in Sec. III, our theoretical derivation only depends on the characteristics of chaotic dynamics and the chunk structure in the Hassell and Ricker model; therefore, we expect that the main results of our paper should hold in other parameter sets whenever these conditions are satisfied.

We calculated multiple trajectories by varying the initial states with fixed parameters. Each trajectory starts from different initial values randomly sampled from a uniform distribution between 0 and 1. The length of each trajectory is set at 20 000 time steps. We eliminated the initial transients (discarded the first 10 000 steps)



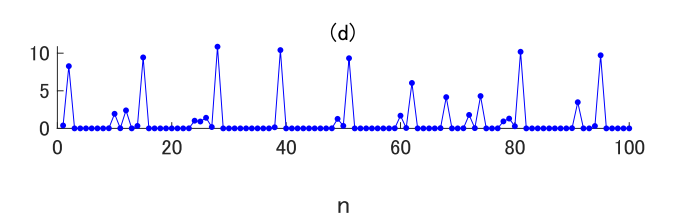


FIG. 1. The chaotic time series of maps used here. (a) Logistic map with r=3.9. (b) Tent map with $\mu=1.9$. (c) Hassell model with $\kappa=10, \nu=12, \lambda=100$. (d) Ricker model with r=5.

and analyzed the last 10 000 steps ($T = 10\,000$). By denoting the nth value of the ith trajectory as x_n^i , we analyzed the ensemble of N samples, computing

$$M_n = \frac{1}{N} \sum_{i=1}^{N} x_n^i,$$

$$V_n = \frac{1}{N} \sum_{i=1}^{N} (x_n^i - M_n)^2$$

for STL and

$$M_i = \frac{1}{T} \sum_{n=1}^{T} x_n^i,$$

$$V_i = \frac{1}{T} \sum_{n=1}^{T} (x_n^i - M_i)^2$$

for TTL (Fig. 2).

The calculation settings of STL and TTL here can be interpreted as the observation of population density at independent multiple places of the equal environmental conditions (e.g., Refs. 9, 20, and 21).

We study the TL relationship in terms of four values as follows: b = cov(M, V)/var(M), var(M), and var(V). The first quantity

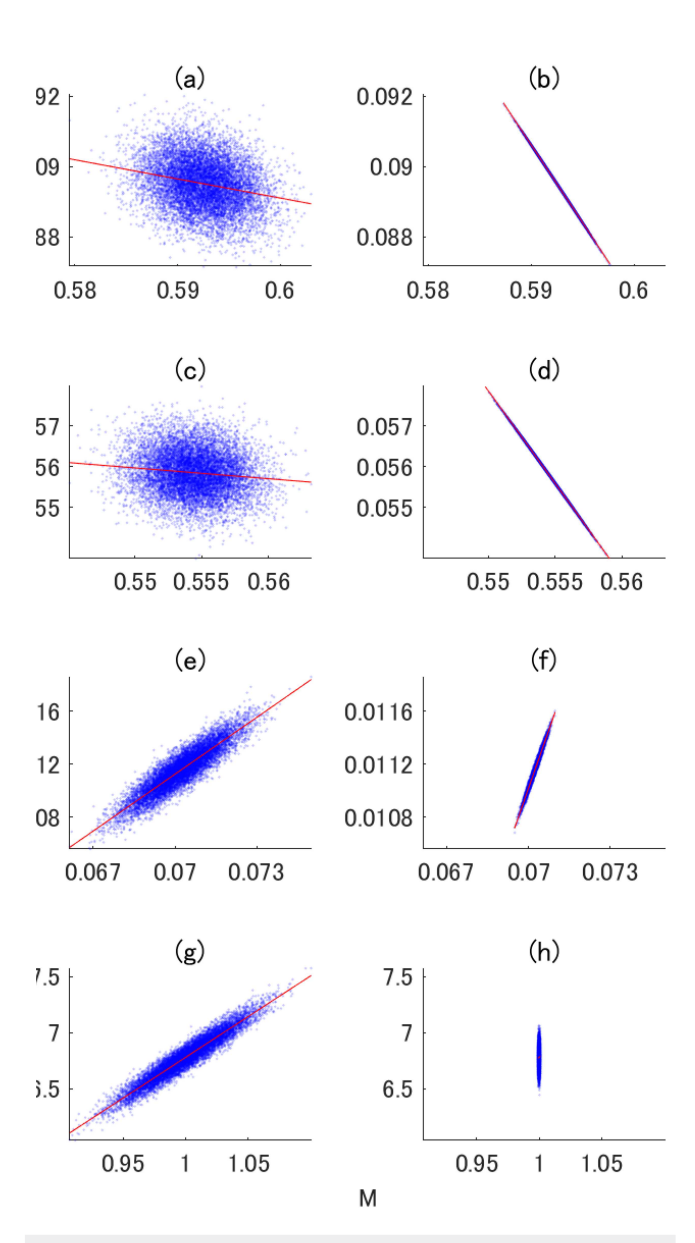


FIG. 2. Results of the numerical simulations of 10 000 sets of (M,V) on the $M\!-\!V$ plane. The data points are represented as blue dots, and the linear regression lines are shown as red lines. (a) STL, logistic map with r=3.9. (b) TTL, logistic map with r=3.9. (c) STL, tent map with $\mu=1.9$. (d) TTL, tent map with $\mu=1.9$. (e) STL, Hassell model with $\kappa=10$, $\nu=12$, $\lambda=100$. (f) TTL, Hassell model with $\kappa=10$, $\nu=12$, $\lambda=100$. (g) STL, Ricker model with $\kappa=10$, $\kappa=10$. (h) TTL, Ricker model with $\kappa=10$.

b corresponds to the slope of the linear regression line on the M-V plane. When the linear regression is valid, this exponent b approximates the exponent β of TL as $\beta \simeq \frac{\overline{M}}{\overline{V}}b$ (\overline{M} and \overline{V} are the sample mean and sample variance calculated over all

trajectories, respectively).²² The calculation details are provided in the supplementary material.

These results are summarized in the "Numerical" columns in Table I, and the box plot of b is shown in Fig. 3.

III. THE ORIGINS OF SPATIAL TL AND TEMPORAL TL

In the following, we will theoretically analyze and reproduce the above arguments.

A. Spatial ensemble

The spatial ensemble is organized by random sampling from a stationary distribution of a given map. The following quantities are given in Refs. 22–24:

$$var(M) = \frac{\mu_2}{N},\tag{5}$$

$$var(V) = \frac{1}{N} \left(\mu_4 - \frac{N-3}{N-1} \mu_2^2 \right), \tag{6}$$

$$cov(M, V) = \frac{\mu_3}{N},\tag{7}$$

where N is the sample size, μ_2 is equal to the variance (or the second central moment) of the stationary distribution, μ_3 denotes the skewness of the stationary distribution (or the third central moment), and μ_4 denotes the fourth moments of the stationary distribution.

The covariance of the sample mean and variance is proportional to the skewness of the distribution. Cohen and Xu^{22} argued that it is one of the possible origins of TL.

In order to confirm that STL is explained from the skewness of the stationary distribution, we computed a stationary distribution from the 10 000 trajectories to calculate μ_2 , μ_3 , and μ_4 . The predicted value matches the value obtained from the numerical calculation, as shown in Table I.

B. Temporal ensemble

TL relationships have different appearances in spatial and temporal ensembles. If each trajectory is independent, spatial TL only depends on the stationary distribution, as stated above, but temporal TL also depends on the temporal structure of the trajectories. We first show how the temporal correlation in trajectories relates to temporal TL; next, we estimate the temporal TL of each map based on the characteristics of each of the temporal structures.

1. A relationship between temporal TL and spatial TL

Equations (5)–(7) only hold when the variables are sampled independently. This holds true for the spatial ensembles but not for the temporal ensembles, as each system has its own characteristic memory length.

We derived that the following generalized equations are applicable when the sample size N is large enough (the derivations are

TABLE I. The results from the numerical simulations ("Numerical") and the predicted values from the theoretical models ("Prediction"). In the "Numerical" column, we calculated the indices from the theoretical models of each map. These results are described with a median and 95% CI calculated from 200 repeated calculations (95% CI is given below the associated median value). The "Chunk" in the Ricker model indicates that the prediction is calculated based on the chunk structure of the dynamics, and the "Formula" indicates that Eq. (11) is used for the prediction in addition to the chunk structure. The calculation details are described in the supplementary material.

		$b = \operatorname{cov}(M, V) / \operatorname{var}(M)$		var(M)		var(V)	
Model	Type	Prediction	Numerical	Prediction	Numerical	Prediction	Numerical
Logistic $(r=3.9)$		-0.056 207	-0.056 188	8.9519*10 ⁻⁶	8.9753*10 ⁻⁶	4.6849*10 ⁻⁷	4.6934*10 ⁻⁷
	Spatial	(-0.056260	(-0.059249	$(8.9508*10^{-6})$	$(8.6127*10^{-6})$	$(4.6844*10^{-7})$	$(4.5432*10^{-7})$
		-0.056149)	-0.053120)	$8.9532*10^{-6}$)	$9.2578*10^{-6}$)	$4.6854*10^{-7}$)	$4.8350*10^{-7}$)
		-0.44142	-0.44132		$1.9021*10^{-6}$		$3.7065*10^{-7}$
	Temporal	(-0.44147	(-0.44151		$(1.8511*10^{-6})$		$(3.6032*10^{-7})$
		-0.44136)	-0.44113)		$1.9562*10^{-6}$)		$3.8131*10^{-7}$)
Tent ($\mu = 1.9$)		-0.027104	-0.026905	$5.5870*10^{-6}$	$5.5960*10^{-6}$	$2.7472*10^{-7}$	$2.7416*10^{-7}$
	Spatial	(-0.027151	(-0.030327	$(5.5859*10^{-6}$	$(5.4148*10^{-6}$	$(2.7466*10^{-7})$	$(2.6625*10^{-7})$
		-0.027060)	-0.023764)	$5.5880*10^{-6}$)	$5.7732*10^{-6}$)	$2.7479*10^{-7}$)	$2.8283*10^{-7}$)
		-0.45362	-0.45348		$1.5664*10^{-6}$		$3.2210*10^{-7}$
	Temporal	(-0.45367	(-0.45367		$(1.5258*10^{-6})$		$(3.1396*10^{-7})$
		-0.45357)	-0.45331)		$1.6127*10^{-6}$)		$3.3160*10^{-7}$)
Hassell ($\kappa = 10, \nu = 12, \lambda = 100$)		0.14187	0.14186	$1.1158*10^{-6}$	$1.1177*10^{-6}$	$2.7672*10^{-8}$	$2.7719*10^{-8}$
	Spatial	(0.14186	(0.14068	$(1.1156*10^{-6})$	$(1.0737*10^{-6}$	$(2.7665*10^{-8})$	$(2.6626*10^{-8})$
		0.14189)	0.14285)	$1.1161*10^{-6}$)	$1.1576*10^{-6}$)	$2.7680*10^{-8}$)	$2.8626*10^{-8}$)
		0.43951	0.58675	$5.0776*10^{-8}$	$4.1391*10^{-8}$	$1.1044*10^{-8}$	$1.4551*10^{-8}$
	Temporal	(0.43690	(0.58500)	$(4.9191*10^{-8})$	$(4.0103*10^{-8})$	$(1.0734*10^{-8})$	$(1.4133*10^{-8})$
		0.44229)	0.58821)	$5.2334*10^{-8}$)	$4.2418*10^{-8}$)	$1.1336*10^{-8}$)	$1.4905*10^{-8}$)
Ricker $(r=5)$		7.2162	7.2193	$6.7806*10^{-4}$	$6.7666*10^{-4}$	0.038743	0.038 667
	Spatial	(7.2151	(7.1719	$(6.7791*10^{-4}$	$(6.5510*10^{-4}$	(0.038 725	(0.037 303
		7.2172)	7.2508)	$6.7820*10^{-4}$)	$7.0472*10^{-4}$)	0.038 759)	0.040184)
		Chunk		Chunk			
		30.484		$1.0273*10^{-6}$			
		(29.099	7.3799	$(1.0035*10^{-6}$	$1.5599*10^{-7}$	Chunk	
	Temporal	31.681)	(3.0874	$1.0589*10^{-6}$)	$(1.5224*10^{-7}$	0.005 067 6	0.0065328
		Formula	11.399)	Formula	$1.5934*10^{-7}$)	(0.0049290	(0.006 373 2
		7.5120		$1.5616*10^{-7}$		0.005 201 3)	0.006 702 1)
		(4.1525		$(1.5217*10^{-7}$			
		11.040)		$1.5962*10^{-7}$)			

provided in the supplementary material):

$$\begin{split} \mathrm{var}(M) &= \frac{\mu_2}{N} + \frac{1}{N^2} \sum_{\tau=1}^{N-1} 2(N-\tau) R_1(\tau), \\ \mathrm{var}(V) &\simeq \frac{1}{N} \left(\mu_4 - \mu_2^2 \right) + \frac{1}{N^2} \sum_{\tau=1}^{N-1} 2(N-\tau) R_2(\tau), \\ \mathrm{cov}(M,V) &\simeq \frac{\mu_3}{N} + \frac{1}{N^2} \sum_{\tau=1}^{N-1} (N-\tau) (R_{12}(\tau) + R_{12}(-\tau)), \end{split}$$

where the first term is equal to Eqs. (5)–(7) when the system size is large. The second order terms are given by the following terms:

$$y_i = x_i - E[x],$$

$$R_1(\tau) = E[y_i y_{i+\tau}],$$

$$R_2(\tau) = E \left[(y_i^2 - \mu_2)(y_{i+\tau}^2 - \mu_2) \right],$$

$$R_{12}(\tau) = E \left[y_i y_{i+\tau}^2 \right].$$

The second order terms will vanish when the variables are uncorrelated. Specifically, the difference between the var(M) values calculated from spatial ensembles and temporal ensembles is proportional to the sum of the auto-correlation function.

We can calculate the TTL if we know $R_1(\tau)$, $R_2(\tau)$, and $R_{12}(\tau)$, but, typically, we need to actually sample the trajectories and directly calculate from them to acquire the functions. Below, we estimate the TTL of each map only using map and conspicuous temporal structure information.

2. Logistic map

The sample mean and variance of the temporal ensembles from the logistic map are strongly correlated [Fig. 2(b)]. We found that

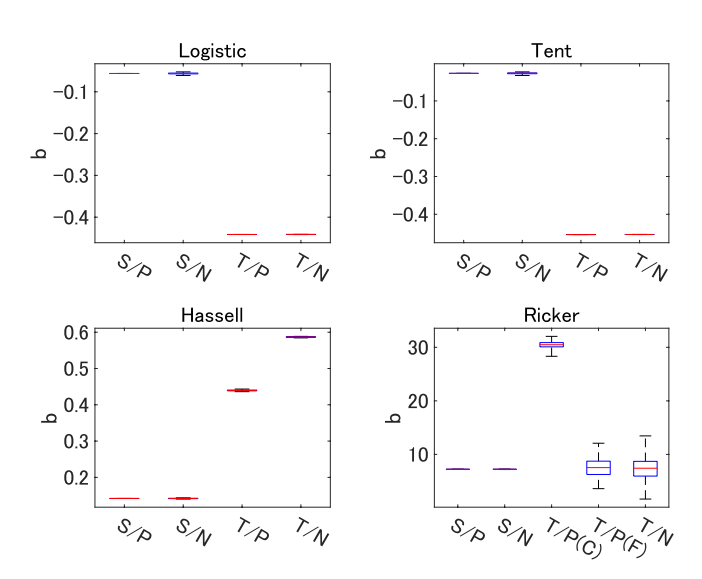


FIG. 3. The results of b of spatial Taylor's law (S) and temporal Taylor's law (T) from the numerical simulations ["Numerical (N)"] and the predicted values from the theoretical models ["Prediction (P)"]. The labels S, T, P, N, C, and F in the figure mean "spatial," "temporal," "Prediction," "Numerical," "Chunk," and "Formula," respectively. The "Chunk (C)" in the Ricker model indicates that the prediction is calculated based on the chunk structure of the dynamics, and the "Formula (F)" indicates that Eq. (11) is used for the prediction in addition to the chunk structure. Full results are shown in Table I.

this is a direct consequence of the quadratic form of the logistic map [Eq. (1)]. By taking the temporal summation of Eq. (1), we analytically derived the following equation (the derivation is provided in the supplementary material):

$$V = \left(1 - \frac{1}{r}\right)M - M^2. \tag{8}$$

In general, a dynamic system containing a quadratic function $(x_{n+1} = cx_n^2 + dx_n)$ shows this relationship in the temporal ensemble as follows (see the supplementary material):

$$V = \frac{1 - d}{c}M - M^2. \tag{9}$$

The quadratic relationship between the sample mean and variance in general was proposed by Bartlett²⁵ and described as follows:

$$V = pM + qM^2$$
.

Sometimes, this relationship has been compared to TL,^{26,27} and, recently, it was called Bartlett's law.²⁸

This quadratic component is evident when we plot the temporal mean and variance calculated from short trajectories as shown in Fig. 4.

In order to check whether it reproduces the results in Table I, we calculated the exponent b using $\frac{dV}{dM}\Big|_{M=\overline{M}}$ (\overline{M} : sample mean of all values in the $10\,000\times10\,000$ data sets). The result is shown in the column "Prediction" in Table I, and it is well fitted with that in the "Numerical" column.

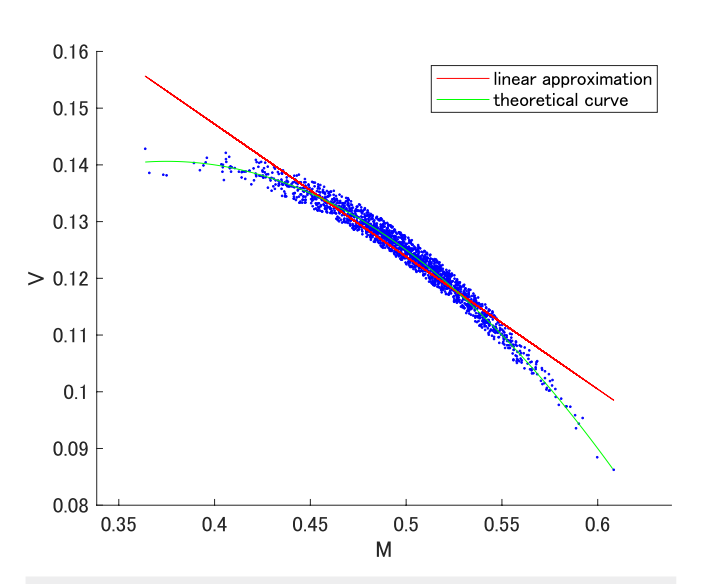


FIG. 4. The typical temporal M–V relationship in the logistic map. Here, r = 4; the number of time steps to calculate the temporal mean and variance is 100, and the number of plots is 2000. The red and green lines represent the linear approximation and the theoretical curve computed from Eq. (8), respectively.

3. Tent map

The TTL of the tent map can also be analytically derived from the equation of the map (the derivation is provided in the supplementary material),

$$V = \frac{\mu}{\mu + 1} M - M^2. \tag{10}$$

This quadratic relation is clearly seen when we plot the temporal mean and variance calculated from short trajectories as well as in the logistic map (Fig. 5).

We calculated b using this equation in the same way as for the logistic map (see the supplementary material), and the result is shown in the column "Prediction" in Table I, which well reproduced the value from the "Numerical" column.

4. Hassell model

The trajectory of the Hassell model in a given parameter region has a chunk structure, in which the value monotonically increases; finally, it abruptly decreased to ~ 0 to start the next chunk (Fig. 1). We assume that this chunk structure is responsible for the M-V relationship in the Hassell model. In order to check the importance of the chunk structures, we reshuffled the temporal ensembles, retaining the chunk structure to build a surrogate ensemble. (The calculation detail is provided in the supplementary material.) The result from the surrogate is shown in the column "Prediction" in Table I. In Table I, the prediction values well reproduced the "Numerical" values

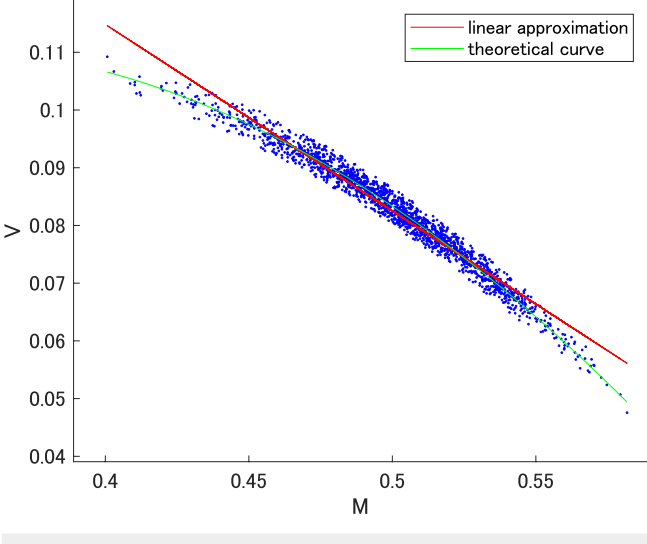


FIG. 5. The typical temporal M–V relationship in the tent map. Here, $\mu=2$; the number of time steps to calculate the temporal mean and variance is 100, and the number of plots is 2000. The red and green lines represent the linear approximation and the theoretical curve computed from Eq. (10), respectively.

5. Ricker model

The time trajectory of the Ricker model in this parameter region also has a chunk structure, but, unlike the Hassell model, the temporal ensemble did not show a correlation in M–V at all, and var(M) is much smaller than the spatial ensemble.

First, we constructed the surrogate ensemble in the same way as the Hassell model. The result is shown in the upper row of the column "Prediction" in Table I. This did not well reproduce the result from the "Numerical" column except for var(*V*).

We found that the discrepancy in var(M) is the direct consequence of the form of the time evolution function, and we analytically showed that the time average depends only on the first term and the (N+1)th term,

$$M = \frac{1}{Nr}(\log x_1 - \log x_{N+1}) + 1,\tag{11}$$

which caused the decorrelation between the sample mean and variance. This relationship can be generalized to the multi-variable stochastic Ricker model used in Ref. 7. The derivations are provided in the supplementary material.

Based on this, we constructed the surrogate ensemble by random sampling two values from the stationary distribution and applying Eq. (11). (The calculation detail is provided in the supplementary material.) The results are shown in the lower row of the column "Prediction" in Table I, and it well reproduced the values in the "Numerical" column.

IV. DISCUSSION AND CONCLUSION

In summary, we have investigated STL and TTL in several chaotic dynamical systems and analyzed the mechanisms of Taylor's law. STL originated from the skewness of the stationary distribution,

which is the same mechanism discussed in Ref. 22, and the difference between STL and TTL was derived from the temporal correlation of the state variables. In our case, each trajectory was independent of each other, and the relationship between STL and TTL only depends on the temporal correlation in each trajectory. Therefore, our results were complementary to past research, ^{12,13} which considered the case of dependent trajectories and argued how the dependence between the trajectories, such as the environmental synchrony and density-dependent dispersal, affected the exponent, although the possibility that the temporal correlation might affect the exponent of TTL was pointed out in Ref. 13.

We also showed that the TTL was well approximated based on the characteristic temporal structure of each map. In the Hassell model, the temporal structure over several time steps, chunk structures, mostly contributed to the M-V relationships, while, in the logistic map and the tent map, the relationships between the present value and the value of the next time step, which are expressed in the time-evolution equations, strongly influenced the mean-variance relationships. Interestingly, while the trajectories from the Ricker model have chunk structures similar to those of the Hassell model, the TTL cannot be well approximated by the chunk structure due to the presence of the relationship directly derived from the map formula [Eq. 11], as found in the logistic map and the tent map.

The quadratic relation obtained for the TTL of the logistic map and the tent map is an example of the relationship called Bartlett's law.²⁵ Our explanation, based on the relationship between the values of consecutive time steps, can provide another explanation for the quadratic relations. On the other hand, the mechanism of TL in high-dimensional systems may be different, and further research is needed.

SUPPLEMENTARY MATERIAL

See the supplementary material for the calculation details of Table I and for details concerning the methods of our numerical simulations and derivations for our analytical results.

ACKNOWLEDGMENTS

The authors would like to deeply thank Joel E. Cohen and Yuzuru Sato for their valuable comments and advice.

DATA AVAILABILITY

The data that support the findings of this study are available from the corresponding author upon reasonable request.

REFERENCES

¹L. R. Taylor, "Aggregation, variance and the mean," Nature **189**(4766), 732–735

(1961).

²C. I. Bliss, "Statistical problems in estimating populations of Japanese beetle larvae," J. Econ. Entomol. **34**, 221 (1941).

³J. E. Cohen, "Statistics of primes (and probably twin primes) satisfy Taylor's law from ecology," Am. Stat. **70**(4), 399–404 (2016).

⁴M. A. De Menezes and A.-L. Barabási, "Fluctuations in network dynamics," Phys. Rev. Lett. **92**(2), 028701 (2004).

⁵Z. Eisler, I. Bartos, and J. Kertész, "Fluctuation scaling in complex systems: Taylor's law and beyond," Adv. Phys. 57(1), 89–142 (2008).

- ⁶R. A. J. Taylor, *Taylor's Power Law: Order and Pattern in Nature* (Academic Press, 2019).
- ⁷A. M. Kilpatrick and A. R. Ives, "Species interactions can explain Taylor's power law for ecological time series," Nature **422**(6927), 65–68 (2003).
- ⁸F. Ballantyne IV, "The upper limit for the exponent of Taylor's power law is a consequence of deterministic population growth," Evol. Ecol. Res. 7(8), 1213–1220 (2005).
- ⁹J. N. Perry, "Chaotic dynamics can generate Taylor's power law," Proc. R. Soc. Lond. B **257**, 221–226 (1994).
- ¹⁰J. E. Cohen, "Taylor's power law of fluctuation scaling and the growth-rate theorem," Theor. Popul. Biol. 88, 94–100 (2013).
- ¹¹L. R. Taylor and I. P. Woiwod, "Comparative synoptic dynamics. I. Relationships between inter- and intra-specific spatial and temporal variance/mean population parameters." J. Anim. Ecol. 51(3), 879–906 (1982).
- population parameters," J. Anim. Ecol. 51(3), 879–906 (1982).

 12T. Saitoh, "Effects of environmental synchrony and density-dependent dispersal on temporal and spatial slopes of Taylor's law," Popul. Ecol. 62, 300–316 (2020).
- ¹³ L. Zhao, L. W. Sheppard, P. C. Reid, J. A. Walter, and D. C. Reuman, "Proximate determinants of Taylor's law slopes," J. Anim. Ecol. 88(3), 484–494 (2019).
- ¹⁴M. P. Hassell, "Density-dependence in single-species populations," J. Anim. Ecol. 44(1), 283–295 (1974).
- ¹⁵M. P. Hassell, J. H. Lawton, and R. M. May, "Patterns of dynamical behaviour in single-species populations," J. Anim. Ecol. 45(2), 471–486 (1976).
- ¹⁶W. E. Ricker, "Stock and recruitment," J. Fish. Res. Board Can. 11(5), 559–623 (1954).
- ¹⁷P. A. P. Moran, "Some remarks on animal population dynamics," Biometrics **6**(3), 250–258 (1950).

- ¹⁸R. M. May and G. F. Oster, "Bifurcations and dynamic complexity in simple ecological models," Am. Nat. **110**(974), 573–599 (1976).
- ¹⁹J. D. Murray, *Mathematical Biology: I. An Introduction* (Springer, 2007).
- 20]. E. Cohen, M. Xu, and W. S. F. Schuster, "Stochastic multiplicative population growth predicts and interprets Taylor's power law of fluctuation scaling," Proc. R. Soc. B: Biol. Sci. 280(1757), 20122955 (2013).
- ²¹J. E. Cohen, "Taylor's law and abrupt biotic change in a smoothly changing environment," Theor. Ecol. 7(1), 77–86 (2014).
- ²²J. E. Cohen and M. Xu, "Random sampling of skewed distributions implies Taylor's power law of fluctuation scaling," Proc. Natl. Acad. Sci. U.S.A. 112(25), 7749–7754 (2015).
- ²³E. Cho, M. J. Cho, and J. Eltinge, "The variance of sample variance from a finite population." Int. I. Pure Appl. Math. **21**(3), 389 (2005).
- population," Int. J. Pure Appl. Math. 21(3), 389 (2005).

 ²⁴L. Zhang, "Sample mean and sample variance: Their covariance and their (in)dependence," Am. Stat. 61(2), 159–160 (2007).
- ²⁵M. S. Bartlett, "Some notes on insecticide tests in the laboratory and in the field," Suppl. J. R. Stat. Soc. 3(2), 185–194 (1936).
- ²⁶L. R. Taylor, I. P. Woiwod, and J. N. Perry, "The density-dependence of spatial behaviour and the rarity of randomness," J. Anim. Ecol. 47(2), 383–406 (1978).
- ²⁷T. B. Swartz and R. D. Routledge, "Taylor's power law re-examined," Oikos **60**(1), 107–112 (1991).
- ²⁸J. E. Cohen, "Every variance function, including Taylor's power law of fluctuation scaling, can be produced by any location-scale family of distributions with positive mean and variance," Theor. Ecol. 13), 1–5 (2020)